Water Resour Manage (2016) 30:3745–3767
DOI 10.1007/s11269-016-1382-y

Evaluating and Calibrating Reference Evapotranspiration Models Using Water Balance under Hyper-Arid Environment

Mohamed A. Mattar[1,4] · **A. A. Alazba**[1,3] · **Bander Alblewi**[2] · **Bahram Gharabaghi**[2] · **Mohamed A. Yassin**[3]

Received: 21 April 2015 / Accepted: 31 May 2016 /
Published online: 8 June 2016

Abstract This research investigates five reference evapotranspiration models (one combined model, one temperature-based model, and three radiation-based models) under hyper-arid environmental conditions at the operational field level. These models were evaluated and calibrated using the weekly water balance of alfalfa by EnviroSCAN to calculate crop evapotranspiration (ET_c). Calibration models were evaluated and validated using wheat and potatoes, respectively, on the basis of weekly water balance. Based on the results and discussion, the FAO-56 Penman-Monteith model proved to be superior in estimating ET_c with a slight underestimation of 2 %. Meanwhile, the Hargreaves-Samani (HS) model (temperature-based) underestimated ET_c by 20 % and the Priestley-Taylor (PT) and Makkink (MK) models (radiation-based) had similar performances underestimating by up to 35 % of the measured ET_c. The Turc (TR) model had the lowest performance compared with other models, demonstrating values underestimated by up to 60 % of the measured ET_c. Local calibration based on alfalfa evapotranspiration measurements was used to rectify these underestimations. The surprisingly good performance of the calibrated simple HS model, with a new coefficient 0.0029, demonstrated its favorable potential to improve irrigation scheduling. The MK and PT models were in third and fourth rank, respectively, reflecting minor differences between one another. The new coefficients obtained for the MK and PT models were 1.99 and 0.963,

✉ Mohamed A. Mattar
mmattar@ksu.edu.sa; dr.mohamedmattar@gmail.com

[1] Agricultural Engineering Department, College of Food and Agriculture Sciences, King Saud University, PO Box 2460, Riyadh 11451, Saudi Arabia

[2] School of Engineering, University of Guelph, N1G 2W1, Guelph, ON, Canada

[3] Alamoudi Water Chair, King Saud University, PO Box 2460, Riyadh 11451, Saudi Arabia

[4] Agricultural Research Center, Agricultural Engineering Research Institute (AEnRI), PO Box 256, Giza, Egypt

respectively. One important observation was that the calibrated TR model performed poorly, with an increase in its coefficient from 0.013 to 0.034 to account for hyper-arid environmental conditions; moreover, it required additional seasonal calibration to adequately improve its performance.

Keywords Crop evapotranspiration · Penman-Monteith · EnviroSCAN · Hyper-arid climate

1 Introduction

Evapotranspiration (ET) is the main factor responsible for the loss of water for use in agriculture around the world, and plays a vital role in the hydrological cycle (Jensen et al. 1990). ET is a joint term that refers to the transfer of water to the atmosphere via evaporation from the soil surface and transpiration from plant tissues (Allen et al. 1998). The three primary factors that affect ET are weather parameters (i.e., temperature, solar radiation, humidity, and wind speed), crop factors (i.e., crop type, variety, and plant density), and management and environmental factors (i.e., soil salinity, poor land fertility, etc.) (Jensen et al. 1990; Allen et al. 1998). Methods of lysimeters and soil water change (water balance) have been used to directly measure ET. These methods, though often expensive and complicated, are effective means of validating and calibrating ET models (Farahani et al. 2007). Mathematical models may also be employed to estimate ET more easily or indirectly when acquisition of measurements is difficult. In this case, a defined surface such as an area of grass or alfalfa is used to estimate ET. ET values acquired using grass as a reference are denoted by the term ET_o, and those acquired using alfalfa are denoted by the term ET_r. Crop ET (ET_c) is estimated by multiplying ET_o or ET_r by the dimensionless crop coefficient (K_c), which reflects the crop, climate, or site conditions (Allen et al. 1998).

There are a large number of models used to estimate evaporation ET_o or ET_r, such as those established by Penman (1948); Thornthwaite (1948); Makkink (1957); Turc (1961); Blaney and Criddle (1962), and Priestley and Taylor (1972). These models were derived either through field experiments or theoretically (Jensen et al. 1990). In cases of developing countries where not all meteorological data is available such as Saudi Arabia, it is necessary to use simplified models that incorporate the available meteorological data. These simplified models are favorable (Tabari 2010) and can be classified into the following groups according to climatic parameters: temperature-based, radiation-based, or combination-based (Igbadun et al. 2006).

The combination method involves application of the FAO-56 Penman-Monteith (FPM) model, which has several advantages similar to those of the lysimeters method under different conditions (Jensen et al. 1990), and is a highly physically-based approach (Irmak et al. 2003). This method also has a number of disadvantages including that it requires a large quantity of meteorological data, requires several assumptions, and results in inaccurate climate parameters with the exception of air temperature (Droogers and Allen 2002; Debnath et al. 2015). Temperature-based methods such as Thornthwaite (TH), Blaney-Criddle (BC), and Hargreaves-Samani (HS) models, are beneficial in that they only require air temperature; however, local calibration is required and the models are highly sensitive to sensible heat advection (Gavilán et al. 2006). Radiation-based methods, such as Priestley-Taylor (PT), Makkink (MK), Turc (TR), and Jensen-Haise (JH) models, require air temperature and radiation. The disadvantages of this method are that local calibration is required (Jensen

1966), it is less sensitive to the accuracy of climate parameters (Hansen 1984), it is only applicable to long period calculations, and it does not account for aerodynamic resistance (Amatya et al. 1995).

Temperature-based models are used all over the world because of their simplicity. The performance of temperature-based approaches differs depending on the kind of the model selected. For example, TH and BC models have superior performance in humid climates (Bautista et al. 2009). Moreover, the HS model demonstrates exceptional performance in semi-arid and arid areas (López-Urrea et al. 2006) and poor performance in a humid environments (Yoder et al. 2005). Therefore, all temperature-based models require calibration between uses in different environments.

The radiation-based models' performances differ from under- or over-prediction depending on the environment in which they are applied. For instance, the PT model overestimates ET_o in humid environments (Yoder et al. 2005; Suleiman and Hoogenboom 2007) while demonstrating excellent performance in Germany (Xu and Chen 2005). Furthermore, the TR models has proven to perform well in humid regions (Yoder et al. 2005). Many radiation-based models are not recommended for use in semi-arid environments (Berengena and Gavilan 2005; Trajković and Gocić 2010). However, PT performed well in a semi-arid environment (Stannard 1993). The JH model is the only radiation model recommended for use in arid regions (Ismail 1993; Mustafa et al. 1989; Alazba et al. 2003).

A number of studies have been conducted in Saudi Arabia, focusing on the Central and Eastern regions to measure and compare the ET_c readings with global records. Moreover, non-weighing lysimeters (Saeed 1988; Mohammad 1997; Al-Ghobari 2000; Alazba et al. 2003; Al-Omran et al. 2004) and pan evaporation (Al-Taher and Ahmed 1992; Ismail 1993) of measuring ET_c have been employed to evaluate and calibrate ET_o models since the 1980s. The ET_o models differ in their performance spatially and temporally. For instance, Mohammad (1997) and Al-Omran et al. (2004) found the Penman models to demonstrate superiority in estimating ET_o whereas Ismail (1993); Mustafa et al. (1989) and Alazba et al. (2003) all found the JH model to be the best. Recently, the FPM model has gained popularity in Saudi Arabia (ElNesr and Alazba 2010; ElNesr et al. 2011) since it is recommended by the Food and Agriculture Organization (FAO). Due to the circumstantial variation in the performance of the different models, it is advisable to continuously study the measurements and estimations of ET_c. Therefore, the aims of this study were to evaluate ET_o models at a field level, calibrate the ET_o models based on measurements, evaluate the accuracy of the calibrated models, and finally, recommend the best model for estimating ET_c in Saudi Arabia.

2 Materials and Methods

2.1 Description of Site

The experimental data was collected from a farm (area of 100 km^2) in Wadi Al–Dawasir, Saudi Arabia. The study area was located between a latitude of 19°56′05.14″ N and 20°00′30.63″ N and a longitude of 44°45′54.60″ E and 44°51′58.07″ E at an elevation of 770 m above sea level. The farm included 90 center pivots. Each pivot had its own well. The farm that was used grows crops of alfalfa, wheat, and potato, which are categorized as economic crops.

2.2 Field Instrumentations and Measurements

The field instrumentations and measurements are displayed for the purpose of collecting data to measure and estimate ET_c. To measure ET_c, the amount of water applied, the soil water content, and crop type were used, whereas to calculate ET_c mathematically, climate data and crop type were used. The inflow rate per month was measured using an ultrasonic device. The areas covered by center pivot were 60 ha, 66 ha, and 45 ha for alfalfa, wheat, and potatoes respectively. The time revolution and water applied were determined on a monthly basis. The time revolution ranged from 18 to 30 h and 30 to 40 h during the winter and summer, respectively. Therefore, the water application and the inflow rate varied accordingly during the season.

The soil texture, bulk density (ρ_s), field capacity (FC), wilting point (WP), and saturation (S) were determined by taking soil samples at four levels (0–20 cm, 20–40 cm, 40–60 cm and 60–80 cm). The soil had a sandy texture (14 % clay, 20 % silt and 66 % sand) and the ρ_s was 1.5 g/cm^3. The soil water content at the FC was 0.206 cm^3/cm^3, at the WP was 0.062 cm^3/cm^3, and at the S was 0.36 cm^3/cm^3.

The EnviroSCAN capacitance probes have the ability to monitor volumetric soil water content (θ_v) continuously at different depths in the root zone. The EnviroSCAN determines when and how much to irrigate. Hence, the EnviroSCAN was used in this study for measuring θ_v at different depths for three locations (i.e. alfalfa, wheat, and potato fields), where the θ_v was one of the components of the water balance method. The probe had five sensors at depths of 10, 20, 30, 50, and 80 cm in the alfalfa field. For the wheat and potatoes fields, the probe had five sensors at depths of 10, 20, 30, 40, and 50 cm. The dynamics of θ_v through time were displayed through the EnviroSCAN software interpolating the frequency readings from the data logger. Sensor readings (field frequencies, F_s) were converted into scaled frequencies (SF) (Buss 1993) as follows:

$$SF = \frac{F_a - F_s}{F_a - F_w} \tag{1}$$

where F_a, F_s, and F_w are the frequency readings of the sensor in air, field, and non-saline water, respectively.

SF is related to θ_v through a standard default calibration equation that provide by the manufacturer of the EnviroSCAN probes as follows:

$$SF = A\theta_v^B + C \tag{2}$$

where A is 0.1957, B is 0.404, and C is 0.02852.

Meteorological data were collected from the climate station. The climatic data involved daily values of the following parameters: maximum, average, and minimum air temperature (T_m, T_a and T_n); maximum, average, and minimum relative humidity (RH_m, RH_a and RH_n); solar radiation (R_s); and wind speed at 2-m height (u_2). Table 1 shows the average monthly weather data in Wadi Al-Dawasir.

Crops of alfalfa, wheat, and potato were selected for ET_c measurement and calculation using weekly water balance and a mathematical approach respectively. Alfalfa is a perennial crop with a root depth of 1 m, while wheat and potatoes are two of the most important irrigated crops in Saudi Arabia. In this study, it was assumed that no ET_c occurred during cutting of the alfalfa. This was decisive when calculating the crop coefficient (K_c) during each cut. Wheat was grown for a period of 120 days; however, only research from the last 10 weeks of growth was used, due to technical

Table 1 Average monthly weather data in Wadi Al-Dawasir

Months	T_m, °C	T_a, °C	T_n, °C	RH_m, %	RH_a, %	RH_n, %	u_2, m/s	R_s, MJ/m^{2}day
JAN	23.4	15.2	7.7	72.2	48.5	26.5	2.50	18.3
FEB	27.6	19.3	11.2	63.9	40.4	22.4	2.75	20.4
MAR	32.4	24.3	16.0	48.1	29.8	18.3	3.07	23.2
APR	34.9	28.2	20.8	53.0	33.2	20.2	3.34	25.4
MAY	38.5	31.2	23.1	48.4	28.2	14.7	2.50	27.5
JUN	41.5	33.5	24.5	35.8	19.1	8.8	2.10	27.5
JUL	41.5	34.6	27.4	36.5	21.7	12.0	2.74	27.8
AUG	42.0	34.8	26.9	35.5	21.2	11.4	2.10	26.0
SEP	38.7	30.6	21.4	39.4	20.9	9.5	2.16	24.7
OCT	34.4	26.5	17.7	49.0	27.8	13.3	1.90	21.3
NOV	26.9	19.2	11.4	61.7	37.8	18.8	1.88	18.9
DEC	22.8	14.8	7.4	65.7	45.5	24.0	2.27	18.0

T_m, T_a, and T_n are maximum, average and minimum temperature; RH_m, RH_a, and RH_n are maximum, average, and minimum relative humidity; u_2 is wind speed; and R_s is Solar radiation

problems affecting the EnviroSCAN during the first 8 weeks. On the other hand, potatoes were grown for a period of 123 days for which all acquired EnviroSCAN data were used.

2.3 Determination of ET_c

Determination of the ET_c was two-fold, comprising the measured water balance model and calculated mathematical model. The water balance model consisted of four parts, net irrigation (I_{net}), effective precipitation (P_e), change in soil water content (ΔS), and deep percolation (D_p) to measure ET_c as residuals. The field water balance of alfalfa, wheat, and potatoes can be defined based on the conservation of mass as follows:

$$\Delta S = I_{net} + P_e - D_p - ET_c \tag{3}$$

where all variables are expressed in mm.

On the other hand, ET_c was estimated mathematically via climatic data collection, valuation of data quality and integrity, calculation of ET_o from the model, and finally, multiplying ET_o by mean the K_c.

2.4 Estimating ET_o

2.4.1 FAO-56 Penman–Monteith (FPM)

The FPM equation for the grass reference crop described by Allen et al. (1998) is as follows:

$$ET_o = \frac{0.408\Delta(R_n - G) + \gamma \frac{900}{T_a + 275} u_2 (e_s - e_a)}{\Delta + \gamma(1 + 0.34u_2)} \tag{4}$$

where ET_o is the reference ET (mm/day), R_n is the net radiation at the canopy surface (MJ/m^2day), G is the soil heat flux at the soil surface (MJ/m^2day), γ is the psychometric constant (kPa /°C), T_a is expressed °C, u_2 is expressed m/s, e_s is the mean saturation vapor-pressure (kPa), e_a is the mean actual vapor-pressure (kPa), $(e_s - e_a)$ is the saturation vapor pressure deficit (kPa), and Δ is the slope of the saturation vapor-pressure–temperature.

2.4.2 Hargreaves-Samani (HS)

The HS model (Hargreaves and Samani 1985) is a modified version of the older ET model presented by Hargreaves and Allen (2003):

$$ET_o = 0.0023R_a(T_a + 17.8)(T_m - T_n)^{0.5} \tag{5}$$

where T_m and T_n are expressed in °C, and R_a is the daily extraterrestrial radiation (mm/day).

2.4.3 Priestley-Taylor (PT)

The PT model (Priestley and Taylor 1972) is a shortened version of the original Penman (1948) model and is defined as follows according to Jensen et al. (1990):

$$ET_o = a\frac{\Delta}{\Delta + \gamma}(R_n - G) \tag{6}$$

where a is an empirical coefficient having a value of 1.26.

2.4.4 Makkink (MK):

The MK model (Makkink 1957) was modified from the Penman equation (Penman 1948):

$$ET_o = 0.61\frac{\Delta}{\Delta + \gamma}\frac{R_s}{\lambda} - 0.12 \tag{7}$$

where R_s is expressed MJ/m^2day, and λ is the latent heat of vaporization (MJ/kg).

2.4.5 Turc (TR)

The TR model (Turc 1961) was developed in Western Europe, as defined for operational use by Allen (2003):

$$ET_o = a_T 0.013\frac{T_a}{T_a + 15}\frac{23.8856R_s + 50}{\lambda} \tag{8}$$

If the average relative humidity is greater than 50 %, then $a_T = 1$. If not, then it can be calculated by $a_T = 1 + \frac{50 + RH_a}{70}$.

2.5 ET_o Model Calibration

The ET_o models required calibration when they did not fit the observed alfalfa ET (ET_r) via the following procedure:

The coefficients of ET_o models were calibrated by using the Microsoft Excel automatic optimization. Xu and Singh (2002) stated that mathematical models can be improved by calibrating the coefficient values of the model. The least square error was used to determine the level of scattering in these models (Castaneda and Rao 2005). The measured ET_r and the computed ET_r were expressed as $(ET_r)_m$ and $(ET_r)_c$, respectively. Setting the conditions and defining the coefficient parameters presented in the models was used to minimize the objective function, which was in turn used to optimize the constant. The minimized function (MF) was achieved using the following equation:

$$MF = \sum \left[(ET_r)_m - (ET_r)_c\right]^2 \tag{9}$$

The calibrated ET_o models were evaluated and validated using wheat and potatoes crops. Eventually, the performance of the models was tested using statistical criteria to identify the best model for irrigation secluding in the Wadi Al-Dawasir environment.

2.6 Models Performance Criteria

Statistical criteria (quantitative) and graphical displays (qualitative) approaches were used to evaluate the performance of the selected ET_o models. In the qualitative approach, data were observed and estimated graphically, while in the quantitative approach, four statistical criteria, the coefficient of determination (R^2), coefficient of efficiency (E), root mean square error (RMSE), and the coefficient of residual mass (CRM) were computed. These statistical performance criteria can be expressed as:

$$R^2 = \frac{\left(\sum_{i=1}^{n}\left(O_i - \overline{O}\right)\left(P_i - \overline{P}\right)\right)^2}{\sum_{i=1}^{n}\left(O_i - \overline{O}\right)^2 \cdot \sum_{i=1}^{n}\left(P_i - \overline{P}\right)^2} \tag{10}$$

$$E = 1 - \frac{\sum_{i=1}^{n}(O_i - P_i)^2}{\sum_{i=1}^{n}\left(O_i - \overline{O}\right)^2} \tag{11}$$

$$RMSE = \sqrt{\frac{\sum_{i=1}^{n}(O_i - P_i)^2}{n}} \tag{12}$$

$$CRM = \frac{\left(\sum_{i=1}^{n} O_i - \sum_{i=1}^{n} P_i\right)}{\sum_{i=1}^{n} O_i} \tag{13}$$

where: O_i and P_i are the observed and estimated values at time step i, respectively; $\overline{O}$ is mean of the observed values; and n is the number of observations.

The R^2 value ranges from 0 to 1, and reflects the degree of correlation between the observed and estimated values. An R^2 value of 1 represents the strongest correlation. The E value ranges from 1 to - ∞. An E value of 1 represents a perfect fit between the observed and estimated values. The RMSE is used to define the difference between the observed values and the model estimations in the same unit of the variable (Licciardello et al. 2007). A model is more accurate if the RMSE value is close to 0. The CRM ranges from −1 to +1, and indicates prevalent model overestimation (i.e. negative values of CRM) or underestimation (i.e. positive values of CRM) of the observed values (Loague and Green 1991; Chanasyk et al. 2003).

2.7 Sensitivity Analysis

Tiberius data mining software, version 7.0.3 was used for the sensitivity analysis to calculate the relative importance of each climatic variables on ET_o for the selected models. The generalized delta rule was used in the training algorithm to develop the artificial neural network (ANN) models (Adamowski 2008). The ANN model contained eight climatic variables, namely, T_m, T_a, T_n, RH_m, RH_a, RH_n, R_s, u_2, as inputs, and one output, ET_o. The optimal ANN architecture was selected by testing a different number of hidden neuron layers. As a result, there were five hidden neurons with the minimum RMSE.

3 Results

3.1 Model Calibration

Figures 1–5 depict the results of the models before and after calibration using an alfalfa crop against $(ET_r)_m$.

3.1.1 FPM Model

Figure 1 shows the weekly averages on a daily basis before and after calibration of FPM ET_r based on 40 weeks of water balance. When $(ET_r)_m$ was greater than 7 mm/day, uncalibrated FPM ET_r was found to be somewhat low, while calibrated FPM ET_r was found to have increased accuracy. However, uncalibrated and calibrated FPM ET_r had 85 % of the data points fall within 99.99 % (red dashed line) of a narrow confidence interval (CI), thereby implying high accuracy. The 1:1 line in Fig. 1 depicts that the uncalibrated and calibrated FPM ET_r fit perfectly with the $(ET_r)_m$. There was less than a 1 % increase of the FPM model's coefficient from 900 to 924. Moreover, the calibrated FPM ET_r improved slightly in estimating ET_r, as shown by Eqs. 14 and 15:

Uncalibrated FPM ET_r:

$$(ET_r)_m = 1.042(\text{FPM } ET_r) - 0.1851 \tag{14}$$

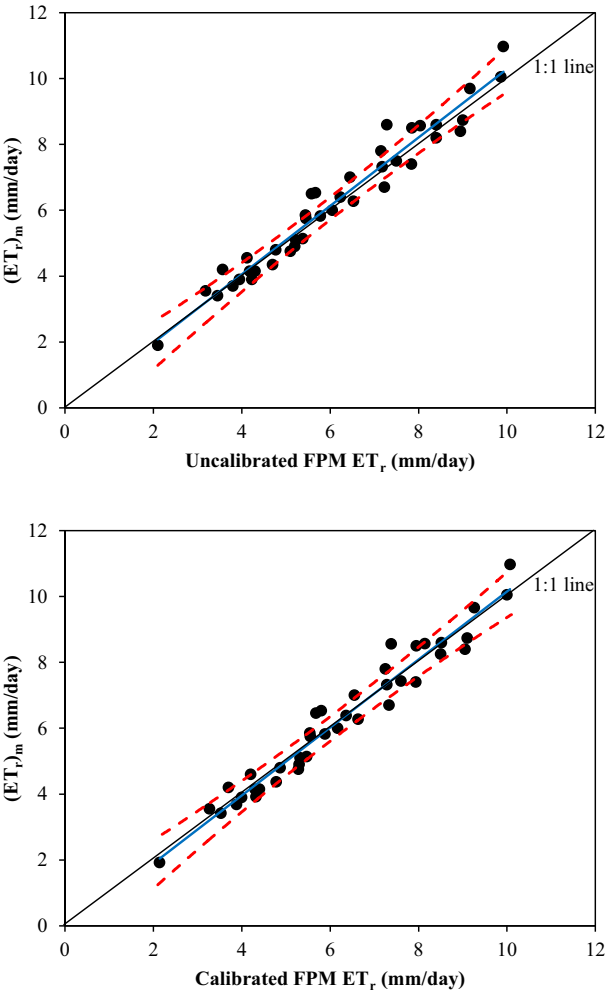

Fig. 1 Regression analysis for the uncalibrated and calibrated FPM ET_r and the $(ET_r)_m$

Calibrated FPM ET_r:

$$(ET_r)_m = 1.027(\text{FPM } ET_r) - 0.1981 \quad (15)$$

In Table 2, the R^2 values indicate a strong positive correlation between the uncalibrated and calibrated FPM ET_r. The values of E for both FPM ET_r models were considered good. The values of RMSE and CRM were close to 0, which indicated that the FPM ET_r performance was sufficiently accurate and performed well without calibration.

3.1.2 HS Model

Figure 2 clearly depicts that the uncalibrated HS ET_r model underestimated the $(ET_r)_m$. Accordingly, calibration was necessary to improve the estimation of ET_r by modifying the model's coefficient. The new coefficient used in the calibrated HS model calibration was equal to 0.0029. This coefficient was 26 % higher than that of the original model's coefficient having

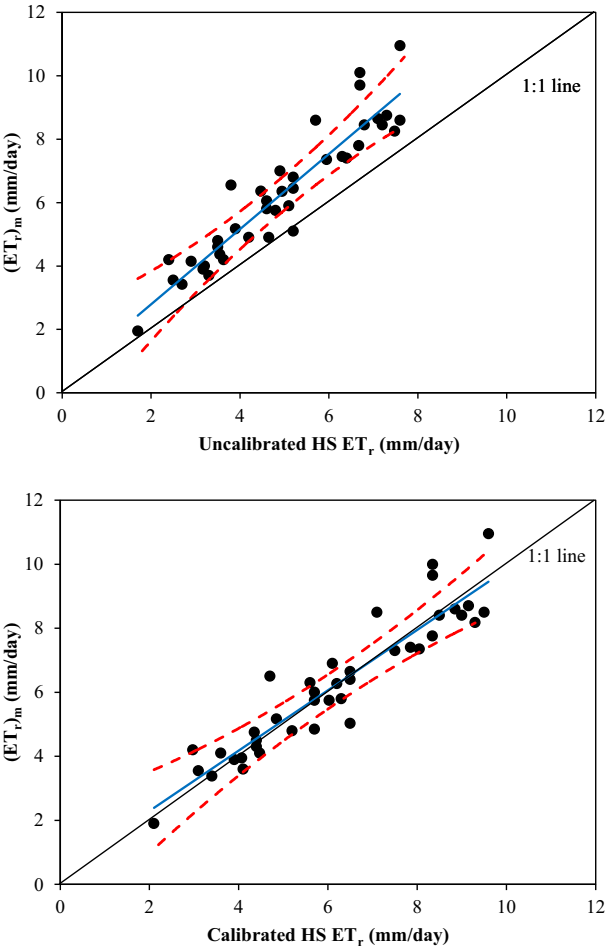

Fig. 2 Regression analysis for the uncalibrated and calibrated HS ET_r and the $(ET_r)_m$

a value of 0.0023. As Fig. 2 depicts the greatly improved match between the calibrated HS ET_r and the $(ET_r)_m$ models. Specifically, 77.5 % of the data points fell within the 99.99 % CI. The regression models were as follows:

Uncalibrated HS ET_r:

$$(ET_r)_m = 1.178(\text{HS } ET_r) + 0.3725 \tag{16}$$

Calibrated HS ET_r:

$$(ET_r)_m = 0.9456(\text{HS } ET_r) + 0.3725 \tag{17}$$

In Table 2, the R^2 values indicate a lack of perfection between uncalibrated and calibrated HS ET_r. For E, the uncalibrated model was considered to be satisfactory ($0.36 \leq 0.48 < 0.75$), while the calibrated model was considered to be good ($0.75 \leq 0.87 \leq 1$). The RMSE and CRM values of the original model were higher than those of the calibrated model. This accentuates the enhancement of the calibrated HS ET_r model in the Wadi Al-Dawasir region.

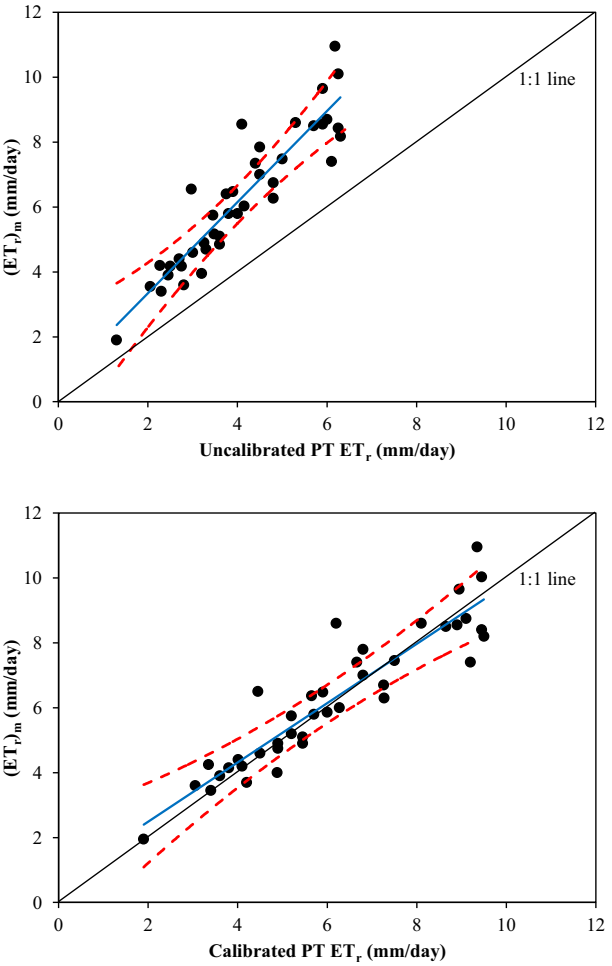

Fig. 3 Regression analysis for the uncalibrated and calibrated PT ET_r and the $(ET_r)_m$

3.1.3 PT Model

The uncalibrated PT ET_r substantially underestimated $(ET_r)_m$ as shown in Fig. 3, thereby identifying its need for calibration in order to yield accurate values of the Wadi Al-Dawasir region. The new coefficient resulting from the calibrated PT model was 1.99, representing a 58 % increase from the original model's coefficient of 1.26. Figure 3 shows that the calibrated PT ET_r fit the $(ET_r)_m$ very well. The 99.99 % CI also shown in Fig. 3 indicates that 80 % of the data points fell inside the interval. The regression model of best fit was as follows:

Uncalibrated PT ET_r:

$$(ET_r)_m = 1.402(\text{PT } ET_r) + 0.535 \tag{18}$$

Calibrated PT ET_r:

$$(ET_r)_m = 0.9218(\text{PT } ET_r) + 0.535 \tag{19}$$

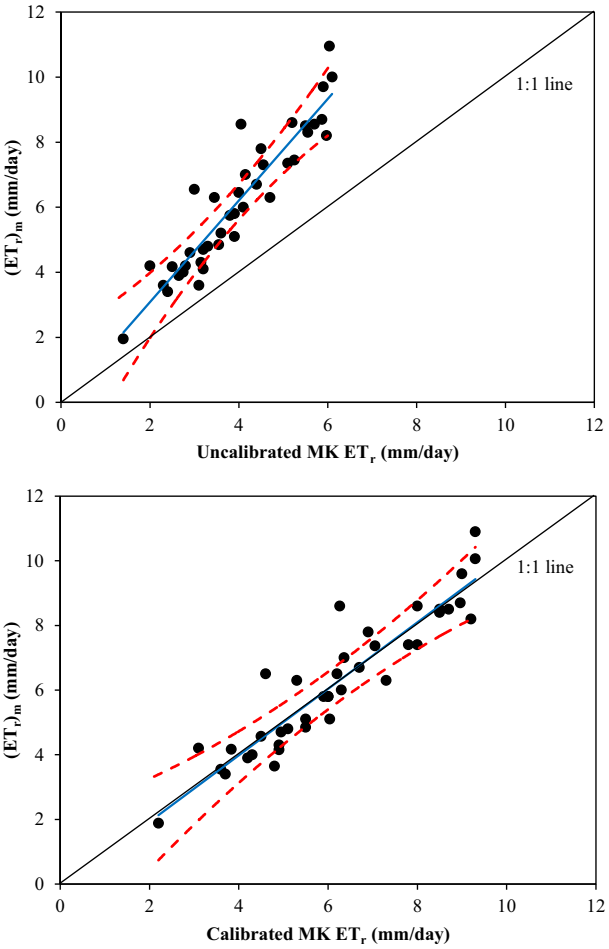

Fig. 4 Regression analysis for the uncalibrated and calibrated MK ET_r and the $(ET_r)_m$

In Table 2, the R^2 values reflected slightly worse performance. For E, the uncalibrated model resulted in poor ET_r estimates ($0.31 < 0.36$) whereas the calibrated model resulted in a better performance ($0.75 \leq 0.85 \leq 1$). The RMSE and CRM indicate that accurate PT ET_r could not be achieved without calibration in the Wadi Al-Dawasir region.

3.1.4 MK Model

Figure 4 visibly indicates that the uncalibrated MK ET_r underestimated $(ET_r)_m$, thereby highlighting the importance of calibrating ET_r to reflect accurate values of the Wadi Al-Dawasir environment, which has expansion of the deviation along the high evaporative demand. The new coefficient derived was 0.963, a 60.5 % increase from the original model's coefficient of 0.6. The regression plot in Fig. 4 depicts that 77.5 % of the data points fell within 99.99 % CI for uncalibrated MK ET_r and calibrated MK ET_r. By looking at Fig. 4, it can be

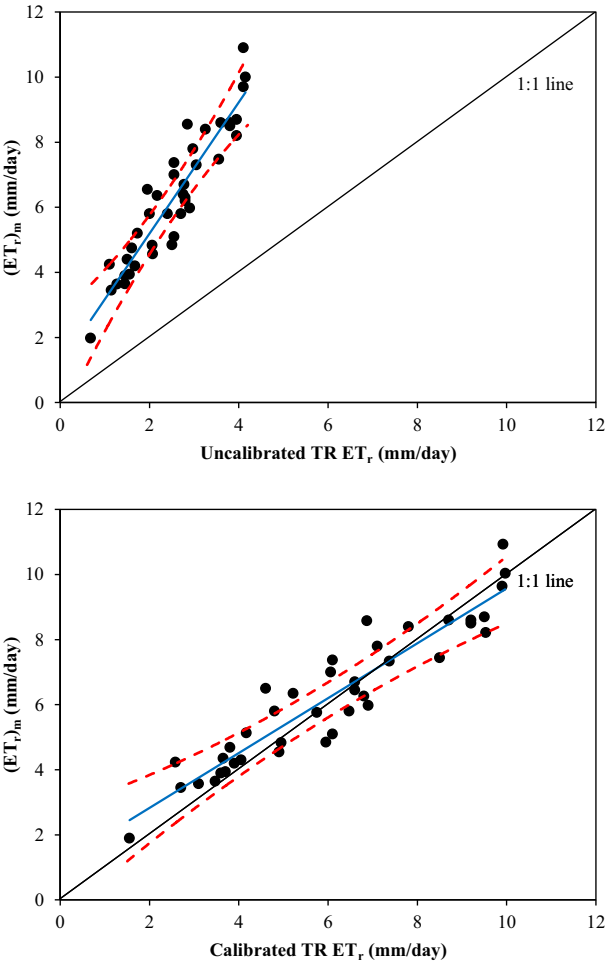

Fig. 5 Regression analysis for the uncalibrated and calibrated TR ET_r and the $(ET_r)_m$

seen that the calibrated MK ET_r fit the $(ET_r)_m$ very well. The regression model of best fit is given by Eqs. 20 and 21:

Table 2 Statistical analysis applied for each tested model before and after calibration on calculating ET_r

$N = 40$ ET_r	Before calibration					After calibration				
	R^2	E	RMSE, mm/day	CRM	Ranked	R^2	E	RMSE, mm/day	CRM	Ranked
PM	0.96	0.95	0.44	0.01	1	0.96	0.96	0.43	−0.004	1
HS	0.87	0.48	1.49	0.20	2	0.87	0.87	0.75	0.01	2
PT	0.85	−0.31	2.37	0.35	3	0.85	0.85	0.82	0.01	4
MK	0.86	−0.33	2.39	0.35	4	0.86	0.86	0.77	0.00	3
TR	0.88	−2.53	3.89	0.60	5	0.88	0.85	0.81	0.02	5

N is Number of weeks

Uncalibrated MK ET_r:

$$(ET_r)_m = 1.574(\text{MK } ET_r) - 0.1706 \quad (20)$$

Calibrated MK ET_r:

$$(ET_r)_m = 1.029(\text{MK } ET_r) - 0.1954 \quad (21)$$

As Fig. 4 indicates, the calibrated MK ET_r had a slope close to 1 and a negative intercept on both models. Table 2 shows that there were no improvements in the R^2 values between calibrated and uncalibrated MK ET_r. For the uncalibrated model, however, the lower value of E was found to be satisfactory ($0.33 < 0.36$), whereas the E value of the calibrated model was found to be good ($0.75 \leq 0.86 \leq 1$). The original model had higher RMSE and CRM values compared to the calibrated model. The E, RMSE, and CRM results confirm the necessity to calibrate the MK ET_r model for the Wadi Al-Dawasir region.

3.1.5 TR Model

Figure 5 clearly shows that the uncalibrated TR ET_r resulted in the greatest underestimation of all the models. The TR model had the lowest data point that fell within the CI at about 62.5 % compared to other models. The TR ET_r model was greatly improved when calibrated as shown in Fig. 5. The new coefficient derived from the calibrated TR model was 0.034, indicating an increase by about 161 % over the original model's coefficient of 0.013. The regression model of best fit was as follows:

Uncalibrated TR ET_r:

$$(ET_r)_m = 2.049(\text{TR } ET_r) + 1.06 \quad (22)$$

Calibrated TR ET_r:

$$(ET_r)_m = 0.8471(\text{TR } ET_r) + 1.06 \quad (23)$$

Table 2 shows that the R^2 values for the uncalibrated and calibrated TR ET_r models indicate a satisfactory fit of the data. For E, however, the uncalibrated model performed poorly ($-2.53 < 0.36$) for estimating ET_r, whereas the calibrated model performed well ($0.75 \leq 0.85 \leq 1$). The RMSE and CRM values for TR ET_r confirmed poor performance without calibration in the Wadi Al-Dawasir region.

3.2 Comparison of ET_o Models

The ET_r were measured and estimated by computing the actual cumulative ET_r, which was the sum of its values over the 40 weeks. Figure 6 compares the five different cumulative models before and after calibration with the $(ET_r)_m$. Before calibration, the ET_r results (1583 mm) on a weekly basis were in excellent agreement with the estimated results from FPM ET_r (1568 mm). Therefore the FPM ET_r was determined to be the best model, followed by the HS ET_r model recording 20 % underestimation of $(ET_r)_m$. On the other hand, the PT ET_r results were similar to those of the MK ET_r having a recorded underestimation of 35 %.

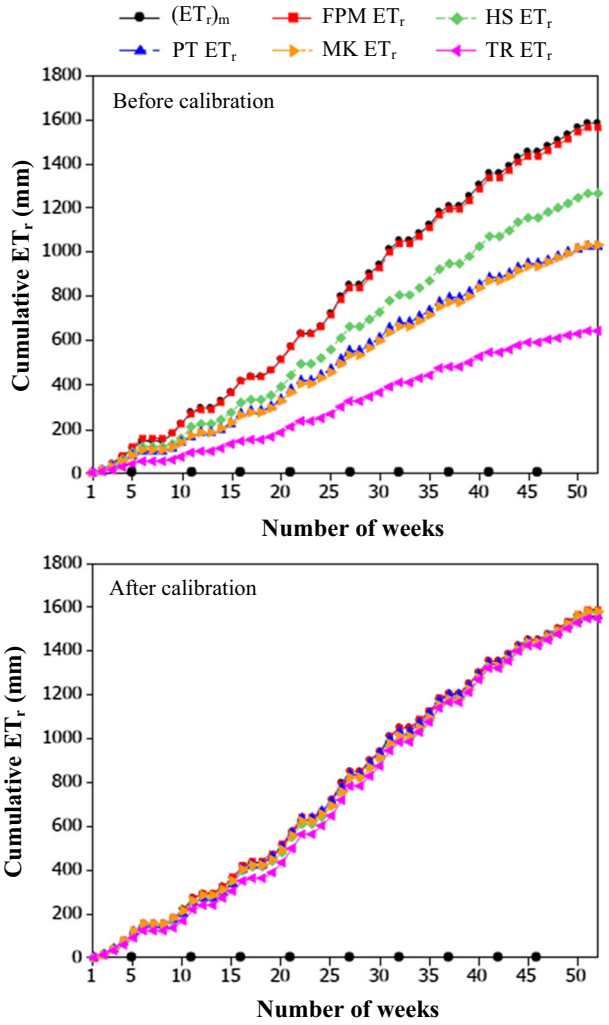

Fig. 6 Cumulative measured and calculated ET_r before and after calibration for 10 cuts period

Finally, the TR ET_r model demonstrated the worst performance with a major underestimation of 60 %. The significantly underestimated values underline the importance of performing calibration when using the radiation and temperature based models within the Wadi Al-Dawasir environmental conditions.

After calibration, performance of all models was greatly improved for the actual cumulative ET_r, as shown in Fig. 6. However, the TR ET_r model required additional seasonal calibration to yield better performance.

3.3 Calibrated Models Evaluation

Figure 7 shows a good match between the observed and calculated wheat ET_c, achieved using the selected models. The FPM ET_c model offered the best performance in estimating wheat ET_c, as confirmed by the R^2 and RMSE values listed in Table 3. The calibrated PT ET_c model lies almost directly atop the 1:1 line with an underestimation of approximately 1 %, indicating

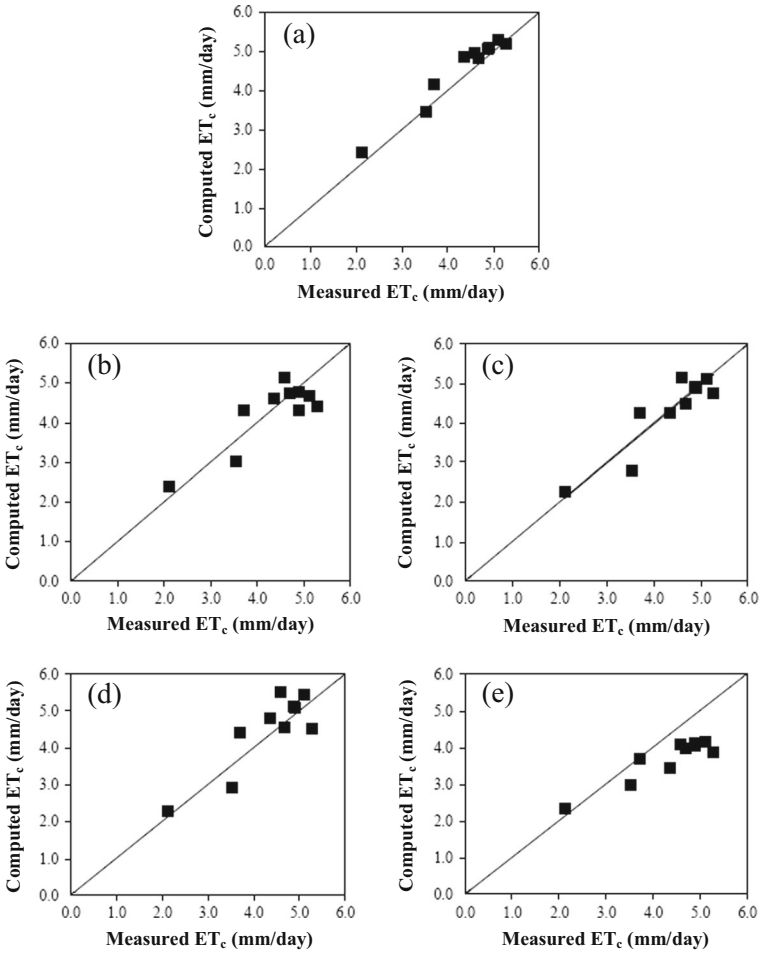

Fig. 7 Scatter plots of measured wheat ET_c with the computed ET_c: (**a**) FPM, (**b**) Calibrated HS, (**c**) Calibrated PT, (**d**) Calibrated MK, and (**e**) Calibrated TR

exceptional agreement with the $(ET_c)_m$. The values of R^2, E, and RMSE (Table 3) indicated that the PT ET_c model performed well following calibration. The CRM for both FPM ET_c and PT ET_c models reflected slight underestimation.

Table 3 Statistical analysis on computing wheat ET_c using different models

$N = 10$ ET_c	R^2	E	RMSE, mm/day	CRM	Ranked
PM	0.95	0.90	0.29	−0.05	1
HS	0.67	0.71	0.49	0.02	3
PT	0.83	0.82	0.38	0.01	2
MK	0.75	0.67	0.52	−0.03	4
TR	0.68	0.25	0.79	0.15	5

N is Number of weeks

The calibrated HS model (Fig. 7) shows the propensity to underestimate (3 %) when increasing demand evaporated beyond the wheat $(ET_c)_m$. As in the FPM ET_c model, the calibrated MK ET_c model recorded a small overestimation (3 %) of $(ET_r)_m$. Table 3 shows that the values of R^2 and E in the HS ET_c and MK ET_c models indicated a moderately positive correlation with $(ET_r)_m$ and the values of RMSE and CRM indicated satisfactory models. The calibrated HS and MK models were ranked third and fourth, respectively in their abilities to accurately estimate wheat ET_c. On the other hand, the calibrated TR ET_c demonstrated the worst performance as reflected by theR^2, E, RMSE, and CRM values (Table 3). Additionally, the TR ET_c model resulted in a 17 % underestimation of $(ET_c)_m$, as shown Fig. 7.

3.4 Calibrated Models Validation

The measured (dashed line) and calculated FPM (solid line) potato ET_c, as shown in Fig. 8, increased with crop development until the beginning of the last third of development, at which values started to decrease. The calibrated HS ET_c model underestimated $(ET_c)_m$ of potato early and late in the potato season, whereas other weeks showed a mixture of over- and underestimated $(ET_c)_m$ values. For example, weeks 5 and 17 yielded underestimated $(ET_c)_m$ values while week 8 yielded overestimated $(ET_c)_m$ values. The highest HS ET_c calculated was 7.25 mm/day while the corresponding value of $(ET_c)_m$ was 6.96 mm/day. Similar to the calibrated HS ET_c model, the calibrated PT ET_c model was used to estimate $(ET_c)_m$ of potato on a weekly basis. The calibrated MK ET_c model overestimated ET_c from weeks 3 to 13, and then underestimation until the season end. The calibrated TR ET_c model demonstrated the worst performance of all the models, as shown in Fig. 8.

In Table 4, the R^2 for FPM ET_c model indicated a robust positive correlation between the observed and estimated ET_c, and a value of E equal to 0.95 confirmed excellent performance. For the HS ET_c, PT ET_c, and TR ET_c models, the R^2 indicated a good fit, whereas for the MK ET_c model, the R^2 confirmed poor performance. The E value for FPM ET_c was 0.95, thereby confirming excellent performance. The PT ET_c model demonstrated similar behavior to that of the HS ET_c model where the E value of PT ET_c was 0.80. Surprisingly, the average of E was 0.74, indicating good and satisfactory MK ET_c model and TR ET_c performance, respectively. The FPM ET_c had the lowest value of RMSE (0.33 mm/day) compared to other models. The corresponding value of HS ET_c indicated good performance. The RMSE value for the PT ET_c model was next best after the HS ET_c model. The TR ET_c model yielded an RMSE value of 0.77 mm/day. The TR ET_c model resulted in similar results to those of the MK ET_c model. The FPM ET_c model had a CRM value of 0.02. This was a minor underestimation of the $(ET_c)_m$. The corresponding value of the HS ET_c model and PT ET_c model was 0.04. The CRM for the MK ET_c model was –0.02 indicating a slight overestimation of $(ET_c)_m$. Finally, the CRM for TR ET_c model indicated a moderate underestimation of $(ET_c)_m$.

3.5 Sensitivity Analysis

Table 5 shows that u_2 and T_m were the most significant parameters affecting the FPM model. Next, R_s had a statistical significance of approximately 0.246 in the FPM model. The temperature was the most influential parameter in the calibrated HS model, while R_s had a smaller effect. For the PT model, R_s was the most important parameter with an equivalency of 100 %. The next most important factor was T_a. The MK and TR models reflected a significant relative importance of R_s, emphasizing the classification of this model as a radiation-based

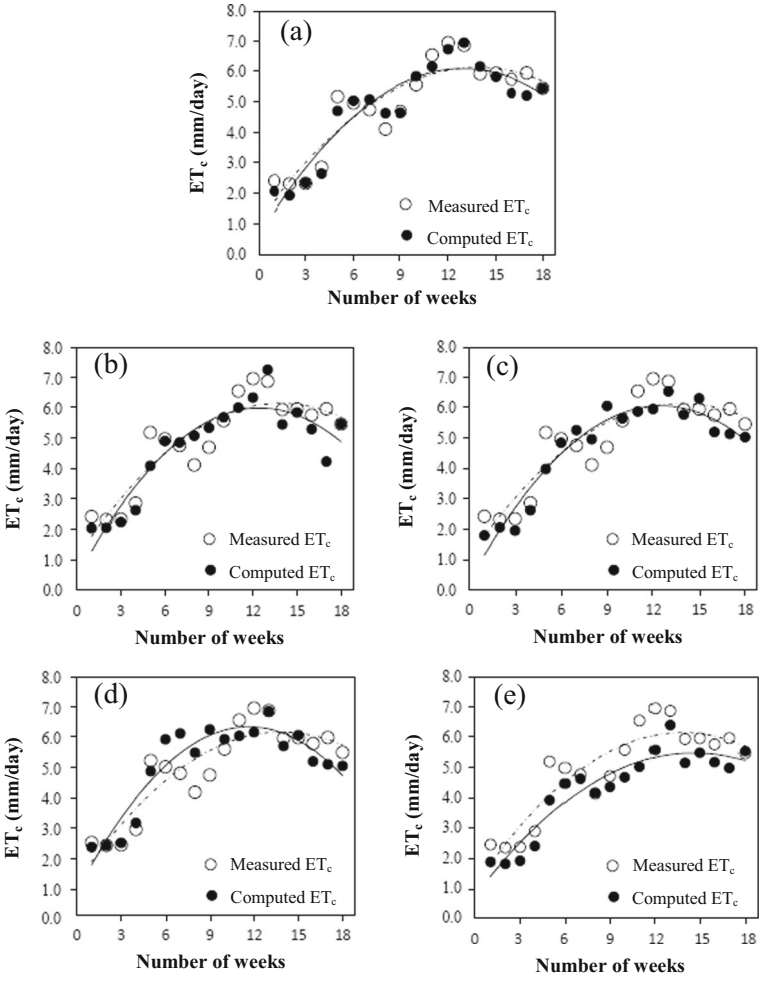

Fig. 8 Comparison of measured potato ET_c with the computed ET_c: (**a**) FPM, (**b**) Calibrated HS; (**c**) Calibrated PT, (**d**) Calibrated MK, and (**e**) Calibrated TR

model. The T_a (of 25 %) in MK model and RH_a (of 88 %) in TR modelwere the second most important parameters.

Table 4 Statistical analysis on computing potato ET_c using different models

$N = 18$ ET_c	R^2	E	RMSE, mm/day	CRM	Ranked
PM	0.97	0.95	0.33	0.02	1
HS	0.77	0.82	0.63	0.04	2
PT	0.83	0.80	0.66	0.04	3
MK	0.64	0.76	0.33	−0.02	4
TR	0.86	0.73	0.77	0.13	5

N is Number of weeks

Table 5 The relative importance of weather data in each tested model

Variables	PM	HS	PT	MK	TR
T_m	0.84	1.00	0.00	0.00	0.00
T_a	0.02	0.81	0.26	0.25	0.54
T_n	0.03	0.27	0.00	0.00	0.00
RH_m	0.03	0.00	0.00	0.00	0.00
RH_a	0.01	0.00	0.00	0.00	0.88
RH_n	0.06	0.00	0.00	0.00	0.00
R_s	0.24	0.17	1.00	1.00	1.00
u_2	1.00	0.00	0.00	0.00	0.00

4 Discussion

The FPM model without calibration was preferable for estimating ET_c in different regions, such as arid regions (Al-Omran et al. 2004; Benli et al. 2006; Dehghani Sanij et al. 2004; Jensen et al. 1990) as shown in the statistical analyses mentioned above. FPM has been used as the standard eq. in many studies to calibrate other empirical equations (Allen et al. 1998; ElNesr et al. 2011; Jensen et al. 1990; Tabari 2010). This implies that ET_c can be measured by EnviroSCAN in spite of its high initial cost and difficult installation. Although FPM is biased, when referring to the ET_r in winter, it highly applicable to wheat ET_c. The sensitivity analysis showed u_2 and T_m to be superior in estimating ET_c in hyper-arid environments. This is consistent with the results of a study conducted by Debnath et al. (2015). Other parameters also had an insignificant influence on ET_c. However, the FPM model has limited application in many regions, such as Wadi Al-Dawasir, because of lack of required climatic data; in addition, it requires trained operators to effectively utilize the FPM model. Under such circumstances, simple alternative equations based on temperature or radiation may be used after calibrating within the local environment.

When the HS model was tested in semi-arid and arid environments, it ranked second to the FPM model (Benli et al. 2010; Nandagiri and Kovoor 2006). In addition, when the difference between the T_m and T_n values (ΔT) was high and u_2 was low, the calibrated HS model demonstrated a maximum overestimation of 29 %, occurring in week 34 (Gavilán et al. 2006). When there was a low ΔT and a high u_2, the calibrated HS model demonstrated a minimum underestimation of 28 %, occurring during weeks 6 and 7 (Gavilán et al. 2006). The ΔT was reduced by decreasing the T_m value during the day and increasing the T_n value at night when the wind mixes the top and bottom atmospheric layers (Temesgen et al. 1999). The u_2 and the ΔT of HS model are very important factors (Razzaghi and Sepaskhah 2011; Tabari and Talaee 2011); howover, the HS model should be calibrated to be used for irrigation scheduling in different environments. Mohammad (1997) reported that the HS model requires calibration in North Saudi Arabia. Generally, the calibrated HS model's performance is good, especially when requiring only T_m and T_n (Allen et al. 1998), thereby improving the estimation of ET_c as reflected by the sensitivity analysis. This provides an advantage for the HS model over other radiation models.

Because of the advection of sensible heat energy in semi-arid and arid regions, the constant α of the PT model range is 1.7–1.75 rather than 1.26, as recommended by Priestley and Taylor (1972). Therefore the PT model should be calibrated in arid regions, as supported by other studies (Jensen et al. 1990; Mohammad 1997). The calibrated PT model's performance ranked

second and fourth for wheat and for alfalfa, respectively. Nandagiri and Kovoor (2006) concluded that the PT model is followed by the HS model in an arid environments, with respect to performance. The calibrated PT ET_r demonstrated good performance from the end of June until early December for alfalfa. While the estimated ET_c values of the first 6 weeks and the last week for wheat overestimated the measured values, and underestimated the measured values during the remaining weeks. A high value of u_2 resulted in underestimation of ET_c during these weeks, representing a positive bias. As in the FPM and HS models, the sensitivity analysis indicated that u_2 and T_m have a tremendous impact on the estimated ET_c by the PT model; therefore, the outlooks were positively and negatively biased.

The MK model demonstrated improved performance when calibrated. Nonetheless, it ranked third after the HS model for alfalfa. Accordingly, it was necessary to calibrate this model seasonally to achieve the best results. As is the case in the alfalfa crop, the MK model of wheat overestimated ET_c during the winter season. The MK model include R_s while the PT model includes R_n, which is difficult to measure. However, the procedure Allen et al. (1998) followed to calculate R_n is adequate, as proven via regression and statistical analyses.

First before each measurement, it was necessary to calibrate the TR model. The TR model underestimated ET_c over the entire duration of the study (Mohammad 1997). Therefore, the TR model was calibrated to appropriately accommodate the Wadi Al-Dawasir environment; however, the problem of its estimation dependency on a seasonal basis remains. As outlined in the previous results, the calibrated TR model demonstrated the worst performance. This indicates that the model must be calibrated seasonally to yield better results. Moreover, the calibrated TR model resulted in poor performance for wheat and potatoes, chiefly during fall and winter. Certainly, use of the TR model led to decreased production due to scarcity of water; therefore, it is not recommended for use in the Wadi Al-Dawasir region. Like radiation-based models, R_s was the most effective variable. On the other hand, RH_a was the second most effective variable which differed from the PT and MK models since the TR model included a relative humidity variable. The least effective variable was T_a when other variables were not considered.

5 Conclusion

This work was used to evaluate and calibrate reference evapotranspiration (ET_o) models by using soil water content probes (EnviroSCAN) on the basis of weekly water balance under hyper-arid environmental conditions. The ET_o models, namely, FAO-56 Penman-Monteith (FPM), Hargreaves-Samani (HS), Priestley-Taylor (PT), Makkink (MK), and Turc (TR) were assessed from estimating crop evapotranspiration (ET_c) of alfalfa water balance in the Wadi Al-Dawasir region. These models were calibrated by minimizing the root mean square error.

The FPM model was the most accurate method for estimating ET_c. We could not apply radiation and temperature-based models in the Wadi Al-Dawasir region due to the associated significant error during their development across different regions. With radiation and temperature-based models, the crop is subjected to water stress resulting in decreased production. Therefore, these models must be calibrated to appropriate account for the Wadi Al-Dawasir environmental conditions. When the empirical models were calibrated to the measured alfalfa evapotranspiration, their performances were significantly improved. Following calibration, the specific ET_o models were evaluated using wheat crops and validated using potato crops. The performance of the calibrated PT model ranked second in estimating wheat

ET_c, followed by the calibrated HS model. The calibrated MK and TR models displayed the worst performances when compared with the measured wheat ET_c, while the calibrated PT and HS models showed the best performance for estimating potato ET_c. The FPM model was found to be the best choice for irrigation scheduling because it includes the most effective variables on ET_c like wind speed, air temperature, and solar radiation. Therefore, the calibrated models can be used with climatic forecasts for better estimation of the irrigation demands on a weekly basis for short-term forecasts. They can be also used with climate variability and change forecasts – long-term climatic – to predict the irrigation water demands.

Acknowledgments With sincere respect and gratitude, we express deep thanks to the Deanship of Scientific Research, King Saud University and Agriculture Research Center, College of Food and Agriculture Sciences, for financial support, sponsorship and encouragement.

References

Adamowski JF (2008) Peak daily water demand forecast modeling using artificial neural networks. J Water Resour Plan Manag 134(2):119–128

Alazba AA, Al-Ghobari HM, Mohammad FS, Alomran AM (2003) Measured and estimated crop ET and Kc for wheat and barley in Central Saudi Arabia. Alex J Agric Res 48(2):1–9

Al-Ghobari HM (2000) Estimation of reference evapotranspiration for southern region of Saudi Arabia. Irrig Sci 19(2):81–86

Allen RG (2003) REF-ET User's guide. University of Idaho Kimberly Research Stations, Kimberly, Idaho

Allen RG, Pereira LS, Raes D, Smith M (1998) Crop evapotranspiration: guidelines for computing crop water requirements. Food and Agriculture Organization of the United Nations, Rome

Al-Omran AM, Mohammad FS, Al-Ghobari HM, Alazba AA (2004) Determination of evapotranspiration of tomato and squash using lysimeter in Central Saudi Arabia. Int Agric Eng J 13(1&2):27–36

Al-Taher AT, Ahmed A (1992) Estimation of potential evapotranspiration in Al-Hassa oasis, Saudi Arabia. GeoJournal 26(3):371–379

Amatya DM, Skaggs RW, Gregory JD (1995) Comparison of methods for estimating REF-ET. J Irrig Drain Eng 121(6):427–435

Bautista F, Bautista D, Delgdao-Carranza C (2009) Calibration of the equation of Hargreaves and Thornthwaite to estimate the potential evapotranspiration in semi-arid and subhumid tropical climates for regional applications. Atmosfera 22(4):331–348

Benli B, Kodal S, Ilbeyi A, Ustun H (2006) Determination of evapotranspiration and basal crop coefficient of alfalfa with a weighing lysimeter. Agric Water Manag 81(3):358–370

Benli B, Bruggeman A, Oweis T, Ustun H (2010) Performance of Penman-Monteith FAO56 in a semiarid highland environment. J Irrig Drain Eng 136(11):757–765

Berengena J, Gavilan P (2005) Reference evapotranspiration estimation in a highly advective semiarid environment. J Irrig Drain Eng 131(2):147–163

Blaney HF, Criddle WD (1962) Determining consumptive use and irrigation water requirements. U. S. Dept. Agr. Agric Res Serv Tech Bull 1275:59

Buss P (1993) The use of capacitance based measurements of real time soil water profile dynamic for irrigation scheduling. Paper presented at the Irrigation 93 Proceeding of the National Conferences of the Irrigation Association of Australia

Castaneda L, Rao P (2005) Comparison of methods for estimating reference evapotranspiration in Southern California. J Environ Hydrol 13:1–10

Chanasyk DS, Mapfumo E, Willms W (2003) Quantification and simulation of surface runoff from fescue grassland watersheds. Agric Water Manag 59(2):137–153

Debnath S, Adamala S, Raghuwanshi NS (2015) Sensitivity analysis of FAO-56 Penman Monteith method for different agro-ecological regions of India. Environ Process 2:689–704

Dehghani Sanij H, Yamamoto T, Rasiah V (2004) Assessment of evapotranspiration estimation models for use in semi-arid environments. Agric Water Manag 64(2):91–106

Droogers P, Allen RG (2002) Estimating reference evapotranspiration under inaccurate data conditions. Irrig Drain Syst 16(1):33–45

ElNesr M, Alazba AA (2010) Simple statistical equivalents of Penman–Monteith formula's parameters in the absence of non-basic climatic factors. Arab J Geosci:1–11
ElNesr MN, Alazba AA, Amin MT (2011) Modified Hargreaves' method as an alternative to the Penman-Monteith method in the kingdom of Saudi Arabia. Aust J Basic Appl Sci 5(6):1058–1069
Farahani HJ, Howell TA, Shuttleworth WJ, Bausch WC (2007) Evapotranspiration: progress in measurement and modeling in agriculture. Trans ASAE 50(5):1627–1638
Gavilán P, Lorite IJ, Tornero S, Berengena J (2006) Regional calibration of Hargreaves equation for estimating reference ET in a semiarid environment. Agric Water Manag 81(3):257–281
Hansen V (1984) Spectral distribution of solar radiation on clear days: a comparison between measurements and model estimates. Clim Appl Meteor 23:772–780
Hargreaves GH, Allen RG (2003) History and evaluation of Hargreaves evapotranspiration equation. J Irrig Drain Eng 129(1):53–63
Hargreaves GH, Samani ZA (1985) Reference crop evapotranspiration from temperature. Appl Eng Agric 1(2): 96–99
Igbadun H, Mahoo H, Tarimo A, Salim B (2006) Performance of two temperature-based reference evapotranspiration models in the Mkoji sub-catchment in Tanzania. Agricultural Engineering International: the CIGR Ejournal, Manuscript LW 05 008. Vol. 8
Irmak S, Allen RG, Whitty EB (2003) Daily grass and alfalfa-reference evapotranspiration estimates and alfalfa-to-grass evapotranspiration ratios in Florida. J Irrig Drain Eng 129(5):360–370
Ismail SM (1993) Reference evapotranspiration study in Al-Qassim region. J Agric Sci 5(2):141–151
Jensen ME (1966) Empirical methods of estimating or predicting evapotranspiration using radiation. Paper presented at the Conference on Evapotranspiration and its Role in Water Resources Management, American Society of Agricultural Engineers
Jensen ME, Burman RD, Allen RG (1990) American society of civil engineers. Committee on irrigation water requirements. Evapotranspiration and irrigation water requirements: a manual. The Society, New York
Licciardello F, Zema DA, Zimbone SM, Bingner RL (2007) Runoff and soil erosion evaluation by the AnnAGNPS model in a small Mediterranean watershed. Trans ASAE 50(5):1585–1585
Loague K, Green RE (1991) Statistical and graphical methods for evaluating solute transport models: overview and application. Journal of Contaminant Hydrology JCOHE6, Vol. 7, No. 1/2, p 51–73, January 1991. 7 fig, 5 tab, 20 ref
López-Urrea R, Olalla FMS, Fabeiro C, Moratalla A (2006) An evaluation of two hourly reference evapotranspiration equations for semiarid conditions. Agric Water Manag 86(3):277–282
Makkink GF (1957) Testing the Penman formula by means of lysimeters. J Institut Water Eng 11(3):277–288
Mohammad FS (1997) Calibration of reference evapotranspiration equations for alfalfa under arid climatic conditions. J King Saud Univ Agric Sci 9(1):39–56
Mustafa MA, Akabawi KA, Zoghet MF (1989) Estimation of reference crop evapotranspiration for the life zones of Saudi Arabia. J Arid Environ 17(3):293–300
Nandagiri L, Kovoor GM (2006) Performance evaluation of reference evapotranspiration equations across a range of Indian climates. J Irrig Drain Eng 132(3):238–249
Penman HL (1948) Natural evaporation from open water, bare soil and grass. Proc R Soc Lond A Math Phys Sci 193(1032):120–145
Priestley CHB, Taylor RJ (1972) On the assessment of surface heat flux and evaporation using large-scale parameters. Mon Weather Rev 100(2):81–92
Razzaghi F, Sepaskhah AR (2011) Calibration and validation of four common ETo estimation equations by lysimeter data in a semi-arid environment. Arch Agron Soil Sci 58(3):303–319
Saeed M (1988) Simple equations for estimating reference evapotranspiration in an arid climate, Saudi Arabia. Arab Gulf J Sci Res 6(3):325–338
Stannard DI (1993) Comparison of Penman-Monteith, Shuttleworth-Wallace, and modified Priestley-Taylor evapotranspiration models for wildland vegetation in semiarid rangeland. Water Resour Manag 29(5): 1379–1392
Suleiman AA, Hoogenboom G (2007) Comparison of Priestley-Taylor and FAO-56 Penman-Monteith for daily reference evapotranspiration estimation in Georgia. J Irrig Drain Eng 133(2):175–182
Tabari H (2010) Evaluation of reference crop evapotranspiration equations in various climates. Water Resour Manag 24(10):2311–2337
Tabari H, Talaee PH (2011) Local calibration of the Hargreaves and Priestley-Taylor equations for estimating reference evapotranspiration in arid and cold climates of Iran based on the Penman-Monteith model. J Hydrol Eng 16(10):837–845
Temesgen B, Allen RG, Jensen DT (1999) Adjusting temperature parameters to reflect well-watered conditions. J Irrig Drain Eng 125(1):26–33
Thornthwaite CW (1948) An approach toward a rational classification of climate. Geogr Rev 38(5):55–94

Trajković S, Gocić M (2010) Comparison of some empirical equations for estimating daily reference evapotranspiration. Arch Civ Eng 8(2):163–168

Turc L (1961) Estimation of irrigation water requirements, potential evapotranspiration: a simple climatic formula evolved up to date. J Ann Agron 12:13–14

Xu CY, Chen D (2005) Comparison of seven models for estimation of evapotranspiration and groundwater recharge using lysimeter measurement data in Germany. Hydrol Process 19:3717–3734

Xu CY, Singh VP (2002) Cross comparison of empirical equations for calculating potential evapotranspiration with data from Switzerland. Water Resour Manag 16(3):197–219

Yoder RE, Odhiambo LO, Wright WC (2005) Evaluation of methods for estimating daily reference crop evapotranspiration at a site in the humid Southeast United States. Appl Eng Agric 21(2):197–202